Supporting Information for

Green synthesis of BiOBr modified $Bi_2O_2CO_3$ nanocomposites with enhanced visible-responsive photocatalytic properties

Nana Guo, Yali Cao*, Yaling Rong, Dianzeng Jia

Key Laboratory of Energy Materials Chemistry, Ministry of Education, Key Laboratory of Advanced Functional Materials, Autonomous Region, Institute of Applied Chemistry, Xinjiang University, Urumqi, Xinjiang 830046, China

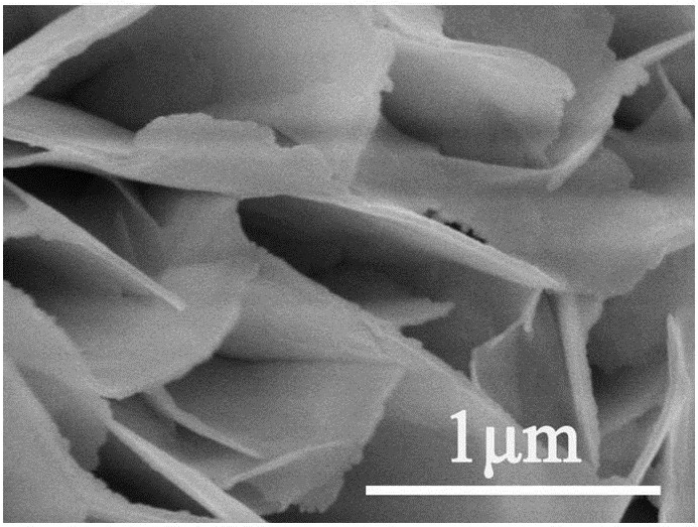

Fig. S1. SEM images of 60% $Bi_2O_2CO_3$/ BiOBr sample.

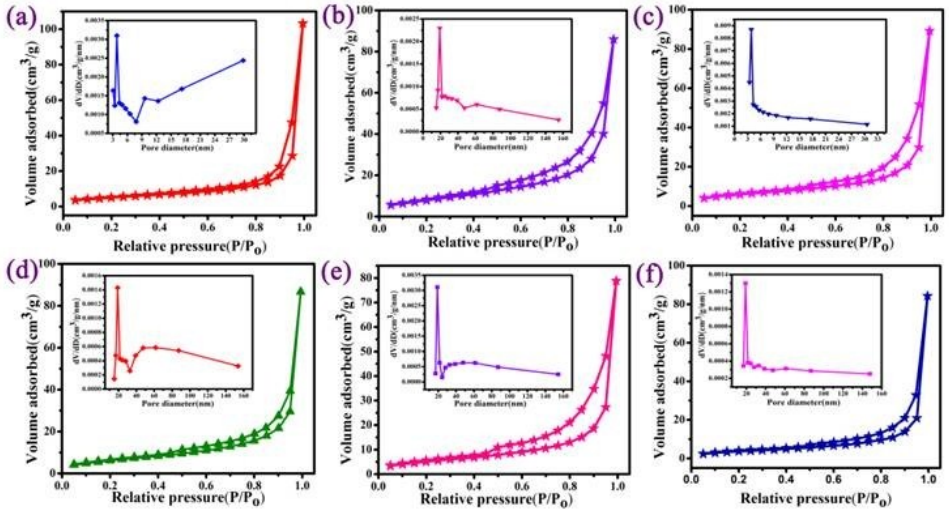

Fig. S2. Nitrogen adsorption-desorption isotherms and pore size distribution for: (a) $Bi_2O_2CO_3$, (b) 20% $Bi_2O_2CO_3$/BiOBr, (c) 40% $Bi_2O_2CO_3$/BiOBr, (d) 60% $Bi_2O_2CO_3$/BiOBr, (e) 80% $Bi_2O_2CO_3$/BiOBr and (f) BiOBr.

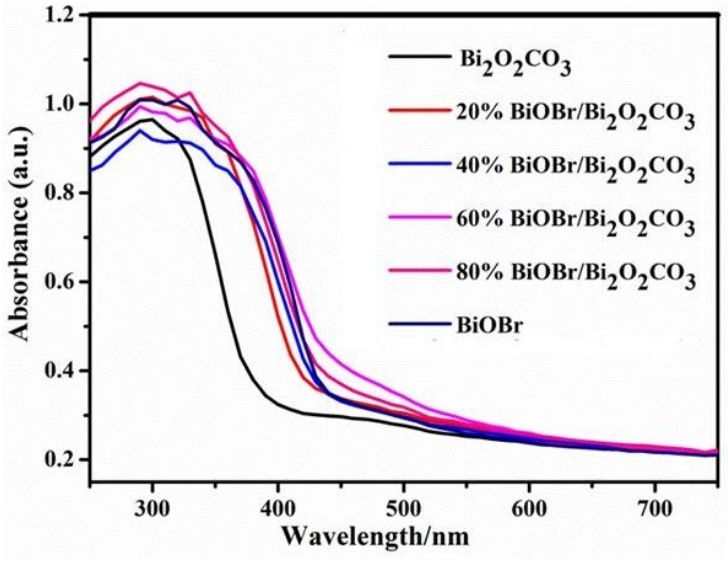

Fig. S3. UV-visible diffuse reflectance spectra of the as-prepared samples.

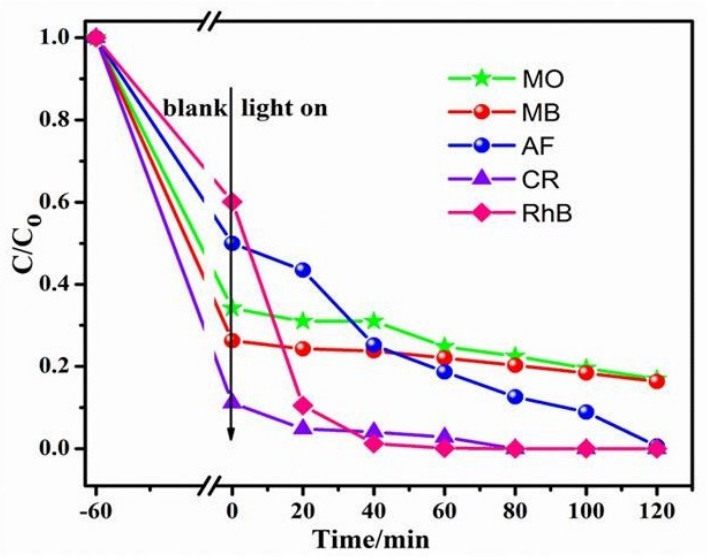

Fig. S4. Photocatalytic degradation curves of 60% $Bi_2O_2CO_3$/ BiOBr sample for methyl orange (MO, 10 mg/L), methyl blue (MB, 20 mg/L), acid fuchsin (AF, 20 mg/L), congo red (CR, 20 mg/L) and rhodamine B (RhB, 20 mg/L) under visible light irradiation.

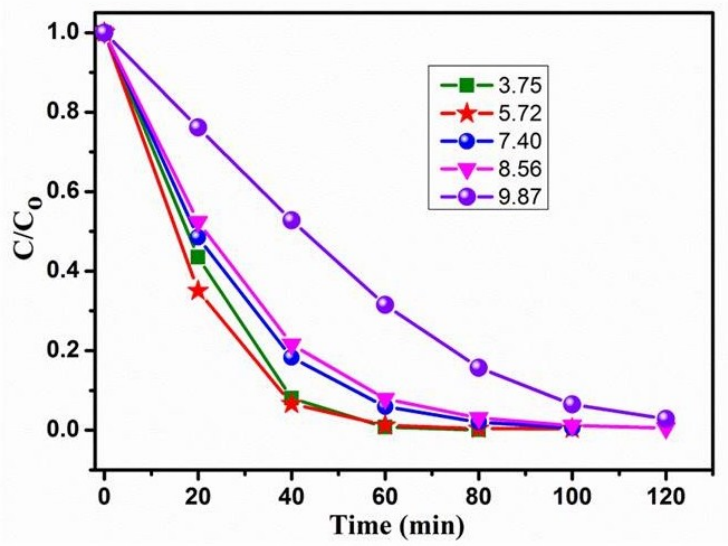

Fig. S5. Photocatalytic degradation curves of RhB solutions with diferent initial pH over 60% BiOBr/$Bi_2O_2CO_3$ sample.

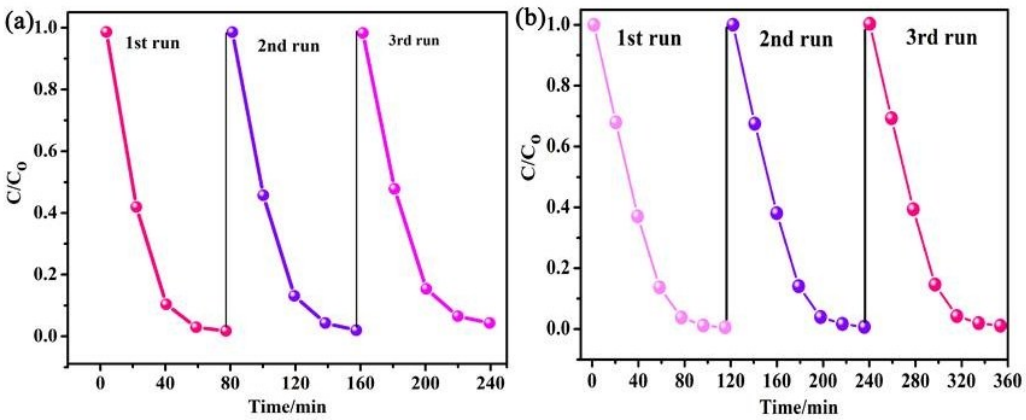

Fig. S6. Cycling runs of (a) 60% BiOBr/$Bi_2O_2CO_3$ and (b) single BiOBr samples under visible-light irradiation.